Theor Chem Acc (2013) 132:1390
DOI 10.1007/s00214-013-1390-4

REGULAR ARTICLE

Theoretical study of the conformational equilibrium of 1,4-dioxane in gas phase, neat liquid, and dilute aqueous solutions

Rute Barata-Morgado · M. Luz Sánchez · Ignacio Fdez. Galván · José C. Corchado · M. Elena Martín · Aurora Muñoz-Losa · Manuel A. Aguilar

Received: 6 March 2013 / Accepted: 8 August 2013

Abstract The conformational equilibrium of 1,4-dioxane in the gas phase, in the pure liquid, and in aqueous solution has been studied by means of the Average Solvent Electrostatic Potential from Molecular Dynamics (ASEP/MD) method and the Integral Equation Formalism for the Polarizable Continuum Model (IEF-PCM). The dioxane molecule was described at the DFT(B3LYP)/aug-cc-pVTZ level. In the three phases, the equilibrium is almost completely shifted toward the chair conformer, with populations of the twist-boat conformers lower than 0.01 %. The equilibrium is dominated by the internal energy of the molecule, as the solute–solvent interaction free energies are very similar in the three conformers considered (chair, 1,4 twist-boat, and 2,5 twist-boat). In the pure liquid, where the dioxane–dioxane interaction is dominated by the Lennard-Jones term, the structure is characteristic of a van der Waals liquid. However, the decrease in the C–H distance from gas phase to solution, the increase in the C–H vibrational frequencies, and the presence of a shoulder in the O–H_{axial} pair radial distribution function point to the presence of a weak C–H–O hydrogen bond. The analysis of the occupancy maps of water oxygen and hydrogen atoms around the 1,4-dioxane molecule confirms this conclusion. Contrary to what is found in small water-dioxane clusters, in the liquid, there is a preference for oxygen atoms to interact with axial hydrogen atoms to form C–H–O hydrogen bonds. Comparison of ASEP/MD and IEF-PCM results indicates that including specific interactions is very important for an adequate description of the solute–solvent interaction; however, the influence of these interactions does not translate in changes in the relative stability of the conformers because it cancels out when energy differences are calculated.

Keywords 1,4-Dioxane · ASEP/MD · QM/MM · Conformational equilibrium · Solvent effect

Electronic supplementary material The online version of this article (doi:10.1007/s00214-013-1390-4) contains supplementary material, which is available to authorized users.

R. Barata-Morgado · M. L. Sánchez (✉) · I. Fdez. Galván · J. C. Corchado · M. E. Martín · A. Muñoz-Losa · M. A. Aguilar
Área de Química Física, Edif. José María Viguera Lobo, Universidad de Extremadura, Avda. de Elvas s/n, 06006 Badajoz, Spain
e-mail: mariluz@unex.es

I. Fdez. Galván
Department of Chemistry, Ångström, The Theoretical Chemistry Programme, Uppsala University, P.O. Box 518, SE-751 20 Uppsala, Sweden

1 Introduction

1,4-Dioxane is a substance that when used as solvent displays an anomalous behavior. So, for instance, it yields solvatochromic shifts that are similar or even larger than those of water although its dielectric constant, 2.21, is very close to the cyclohexane value, a paradigm of non-polar solvent. 1,4-Dioxane has no permanent dipole moment in its predominant chair conformation; however, it has two oxygen atoms with proton–acceptor character, and consequently, it can form intermolecular hydrogen bonds with proton–donor molecules. Furthermore, its charge distribution can be described as two anti-parallel dipoles, each one of them can interact with the dipoles of other dioxane molecules or with the solvent.

Several experimental works [1–4] have analyzed the geometry, structure, dielectric constant, dipole moment, vibrational and electronic spectra, ionization potential, and conformational equilibrium of 1,4-dioxane. To this respect, Takamuku et al. [5] conclude, from the analysis of X-ray data, that 1,4 dioxane is a mixture of 65 % chair and 35 % twist-boat conformers. However, theoretical calculations [6] using this proportion yield a dielectric constant value of 3.34, which is larger than the experimental value. This fact points to a fraction of twist-boat form considerably lower than 35 %. The conformational equilibrium of 1,4-dioxane has been also theoretically studied in gas phase [2, 7], and in neat liquid, in the latter case using dielectric continuum methods [8], classical Monte Carlo [6, 8, 9], and molecular dynamics simulations [10]. In gas phase, a weakly distorted chair form is the most stable conformation, followed by 2,5 twist-boat and 1,4 twist-boat forms that are close to each other in energy but are higher by about 6-7 kcal/mol than the chair form. Other conformations are also possible, but because their energies are significantly higher, their contribution to the conformational equilibrium can be safely neglected. In the liquid, Cinacchi et al. [10] found that the chair form is also the most stable conformation. Only about 1 % is in the 2,5 twist-boat form, although other studies yield even lower populations [6, 8]. Given the dipole moment differences between the conformers, it remains to clarify whether the explicit consideration of the molecular polarization would have some effect on the conformational equilibrium.

The structure of 1,4-dioxane in aqueous solution has been also analyzed. 1,4-Dioxane and water are miscible [11] in any proportion and their mixtures have been profusely used as solvent. Because of the high value of the dielectric constant of water, the differences in the dipole moment of the conformers, and the formation of dioxane-water hydrogen bonds, HBs, one expects that the conformational equilibrium could be different in water solution from the neat liquid. In fact, Pchelkin and Toryanik [12] have stated that the hydration of 1,4-dioxane is energetically more favorable in the boat conformation than in the chair conformation. This behavior would be related with the fact that the 2,5 twist-boat conformer displays gas phase dipole moment values close to 1.5 D, while the chair form is almost non-polar. In solution, these differences can be even larger due to the solute polarization. Consequently, it is expected that the twist-boat conformer becomes stabilized in liquid phase with respect to other conformers.

An important point to clarify is the role that non-conventional C–H–O hydrogen bonds could have on the conformational equilibrium and structure of the liquid. High-pressure infrared and Raman spectroscopy experiments [4, 13] have suggested the presence of these interactions in aqueous 1,3-dioxane and 1,4-dioxane. However, in water-dioxane mixtures, the influence of non-conventional HB on the structure of the solvent is hidden by the presence of O–H–O HBs. This does not occur in the neat liquid where only C–H–O can be formed and where, consequently, it could be easier to find signs of these interactions.

In our study about the conformational equilibrium in 1,4-dioxane, we used a QM/MM method, named *Averaged Solvent Electrostatic Potential from Molecular Dynamics* (ASEP/MD) [14]. This method permits to combine a very precise description of the solute using state of the art quantum mechanics calculations with a detailed, microscopic description of the solvent. The method permits the coupling between the solute charge distribution and the solvent structure around it, and consequently, it becomes possible to study the effect that the solute polarization has on conformational equilibria. ASEP/MD has been successfully applied to the study of the conformational equilibriums in solution of small peptides [15] and hydrocarbons [16] where conventional intermolecular hydrogen bonds play a very important role. We expect that it permits to analyze the subtleties of the conformational equilibrium in liquids such as 1,4-dioxane where non-conventional HBs seem to be present.

Additionally, we study the influence that a dielectric continuum or a molecular mechanics description of the solvent has on the properties and structure of 1,4-dioxane. In their study about coumarin C153 in dioxane using an effective pair potential that includes molecular flexibility, Cinacchi et al. [10] concluded that solvatochromic shifts and solvation dynamics in 1,4-dioxane cannot be accurately studied without considering the molecular detail and the local solvation structure. In this paper, we study the effect that the solvent description has on the conformational equilibrium, HOMO–LUMO energy gap, and ultraviolet absorption spectra of dioxane. It is shown that, unexpectedly, a dielectric continuum model, despite its oversimplified description of the solvent, can yield results comparable to those of more complete models even in the presence of specific interactions.

The rest of the paper is organized as follows: Sect. 2 describes the methodology; we pay special attention to the main features of ASEP/MD and to the procedure followed in calculating solute–solvent free energy contribution. Section 3 displays the computational details. Section 4 presents the results and discussion of the stability of the different conformers in gas phase, in the neat liquid, and in water solution with special emphasis on the formation of conventional and non-conventional hydrogen bonds. Finally, Sect. 5 concludes with a summary of the key points.

2 Methods

Solvent effects on the structure and properties of 1,4-dioxane were calculated with the ASEP/MD method [14].

This is a sequential QM/MM method that makes use of the mean field approximation and in which the perturbation generated by the solvent is introduced into the solute molecular Hamiltonian in an averaged way. Details of the method have been described elsewhere [17–23]. So, here, we will only present a brief outline.

ASEP/MD combines a high-level quantum mechanics (QM) description of the solute with a molecular mechanics (MM) description of the solvent. The solute–solvent configurations are obtained through classical molecular dynamics simulations (MD) of the system. From a selected set of the solvent configurations, the average electrostatic potential generated by the solvent in the volume occupied by the solute is calculated. This potential is introduced as a perturbation into the solute's quantum mechanical Hamiltonian and, by solving the associated Schrödinger equation, one gets a new charge distribution for the solute, which is used in the next MD simulation. This iterative process is repeated until the electron distribution of the solute and the solvent structure around it become mutually equilibrated.

As usual in QM/MM methods, the ASEP/MD Hamiltonian is partitioned into three terms [24–30]:

$$\hat{H} = \hat{H}_{QM} + \hat{H}_{MM} + \hat{H}_{QM/MM} \tag{1}$$

Here, $\hat{H}_{QM}$ corresponds to the quantum part, $\hat{H}_{MM}$ to the classical part, and $\hat{H}_{QM/MM}$ to the interaction between them. In the current study, the quantum part comprises only the solute molecule. The classical part comprises all the solvent molecules.

The energy and wave function of the solvated solute molecule is obtained by solving the Schrödinger equation:

$$\langle\left(\hat{H}_{QM} + \hat{H}_{QM/MM}\right)|\Psi = \langle E|\Psi \tag{2}$$

The interaction term takes the following form:

$$\hat{H}_{QM/MM} = \hat{H}^{elect}_{QM/MM} + \hat{H}^{vdw}_{QM/MM} \tag{3}$$

$$\hat{H}^{elect.}_{QM/MM} = \int \mathrm{d}r \cdot \hat{\rho} \cdot V_s(r; X_i) \tag{4}$$

where $\hat{\rho}$ is the solute charge density operator. The term $V_s(r; X_i)$, is the averaged electrostatic potential generated by the solvent at the position r, and it is obtained from MD simulations in which the solute molecule is represented by the charge distribution, ρ, and the geometry fixed during the simulation. The term $\hat{H}^{vdw}_{QM/MM}$ is the Hamiltonian for the van der Waals interaction, in general represented by a Lennard-Jones potential.

One important feature of ASEP/MD is that it permits to study the relative stability of the different conformers in solution. In calculating free energy differences, we follow a dual-level methodology: the geometry and charges of the different conformers in solution are obtained using quantum mechanical methods, but the solute–solvent free energy contribution is calculated classically. The free energy difference between two conformers, A and B, in solution is written as the sum of two terms [31]:

$$\Delta G = \Delta E_{QM} + \Delta G_{int} \tag{5}$$

where ΔE_{QM} is the difference in the quantum internal energy between the two conformers, and it is calculated using the in solution wave functions; ΔG_{int} is the solute–solvent interaction free energy, which is calculated classically using the free energy perturbation method [32–34]. In turn, the term ΔG_{int} can be divided into two terms: $\Delta G_{int} = \Delta E_{int} + \Delta G_{solv}$. The term ΔE_{int} is the difference of solute–solvent interaction energy between the initial and final state. The last term, ΔG_{solv} provides the solvent distortion energy, i.e., the energy cost in changing the structure of the solvent from the initial state to final one.

In sum, the free energy difference between two conformers A and B reads:

$$\begin{aligned}\Delta G_{A\to B} &= G(r_B) - G(r_A)\\ &= \Delta E_{QM} + k_B T \ln\langle e^{\left[E_{QM/MM}(r_B) - E_{QM/MM}(r_A)\right]}\rangle_i\end{aligned} \tag{6}$$

$$\begin{aligned}\Delta E_{QM} &= E^B_{QM} - E^A_{QM}\\ &= \langle\Psi_B|\hat{H}_{QM,B}|\Psi_B\rangle - \langle\Psi_A|\hat{H}_{QM,A}|\Psi_A\rangle.\end{aligned} \tag{7}$$

In optimizing the solute geometry, we used a variation of the free energy gradient method [35] described elsewhere [20].

3 Computational details

The geometry of the conformers of 1,4-dioxane was optimized using *density functional theory* with the B3LYP functional [36–39] both in gas phase and in solution. The basis set used throughout the study was *aug*-cc-pVTZ. Yang et al. [1] find that this level of calculation reproduces correctly the valence orbital energies obtained by electron momentum spectroscopy. Furthermore, the size of the basis set permits to describe adequately the polarization of the solute during the solvation process. The nature of the minima was checked by means of a frequency calculation, showing that all the vibrational frequencies are real.

In studying the neat liquid, the simulation box was formed by 300 molecules of 1,4-dioxane. We perform several simulations considering different populations of the chair and twist-boat forms. The electrostatic interaction was calculated with the Ewald method, and the temperature was fixed at 298 K with the Nosé-Hoover thermostat. Each simulation was run for 75 ps with a time step of 0.5 fs. From the 150,000 steps, 50,000 were used for equilibration and 100,000 for production. A cubic box of 36 Å was used. Periodic boundary conditions were applied and a spherical cutoff was used to truncate the solute–solvent and solvent–

Table 1 Intermolecular Lennard-Jones parameters

	σ (Å)	4ε (kcal/mol)
O (Dioxane)	3.00	0.680
C (Dioxane)	3.80	0.472
O (Water)	3.15	0.608

solvent interactions at 12.9 Å. The Lennard-Jones parameters [9] in 1,4-dioxane molecule are displayed in Table 1. During the molecular dynamics simulation, all the molecules were considered rigid. Final results (energies, charges, and RDFs) were obtained by averaging the last five ASEP/MD cycles, and therefore, they represent a 250 ps average.

In studying 1,4-dioxane-water solutions, the simulations contain one 1,4-dioxane molecule and 500 water molecules in a cubic box of 24.7 Å. As in the neat liquid, the simulation was conducted during 150,000 steps of 0.5 fs duration. A spherical cutoff of 10.5 Å side was used to truncate the molecular interactions. For water molecules, the TIP3P [40] model was used.

The in solution calculations were performed using a version of the ASEP/MD, which uses GAUSSIAN-09 [41] for the quantum calculations and MOLDY [42] to carry out the simulation processes. When necessary, the atomic charges were calculated using the CHELPG (*Charges from Electrostatic Potential in a Grid*) method [43, 44].

Continuum dielectric calculations were performed with the IEF-PCM [45] as implemented in GAUSSIAN-09 using as cavity radii 1.2 times the van der Waals radii.

4 Results and discussion

4.1 Gas phase

Previous gas phase studies [7] have evidenced that the three most stable conformers of 1,4-dioxane are a weakly distorted chair structure and the 2,5 twist-boat and 1,4 twist-boat forms, see Fig. 1.

At the B3LYP/aug-cc-pVTZ level, the free energy differences between the chair and the 2,5 twist-boat and the 1,4 twist-boat forms are 6.1 and 5.7 kcal/mol, respectively (6.8 and 6.4 kcal/mol if only potential energy differences are considered). Our results slightly disagree with those obtained by other authors. So, for instance, Chapman and Hester [7] found that at the BLYP/6-31G* level, the relative stability order of the twist-boat conformers is reversed, while at the MP2/6-31G* level, the two isomers have the same stability. These authors [7] also find a 1,4-boat (C_{2v}) form with energy similar to the 2,5 twist-boat form, but at B3LYP/aug-cc-pVTZ level that structure was not a minimum. In order to clarify this point, we reoptimized the different structures at MP2 level. The results for the relative stability of the three conformers above considered, 7.0 and 6.6 kcal/mol, agreed with our B3LYP results. At MP2 level, the 1,4-boat (C_{2v}) form becomes now a real minimum, but with such a large energy, 9.1 kcal/mol, with respect to the chair form, it does not contribute to the gas phase conformational equilibrium. Some other conformers have been found but they are placed at significantly higher energies, and therefore, they will not be considered here.

With respect to the charge distribution, the chair and 1,4 twist-boat forms have null dipole moment, while the 2,5 twist-boat has a dipole moment of 1.51 D (see Table 2). It is worth noting that the atomic charges are very similar in chair and boat conformers, and consequently, the differences in the dipole moment are due to the relative orientation of the partial dipoles rather than to differences in the charge distribution of the conformers. In fact, the charge distribution of the molecule can be considered as formed by two partial dipoles that in the chair and 1,4 twist-boat, conformers are anti-parallel, while in the 2,5 twist-boat, conformer forms an angle of 116°.

4.2 Neat liquid

4.2.1 Thermodynamics

We start this section by analyzing the relative stability of the different conformers in the neat liquid, see Table 3.

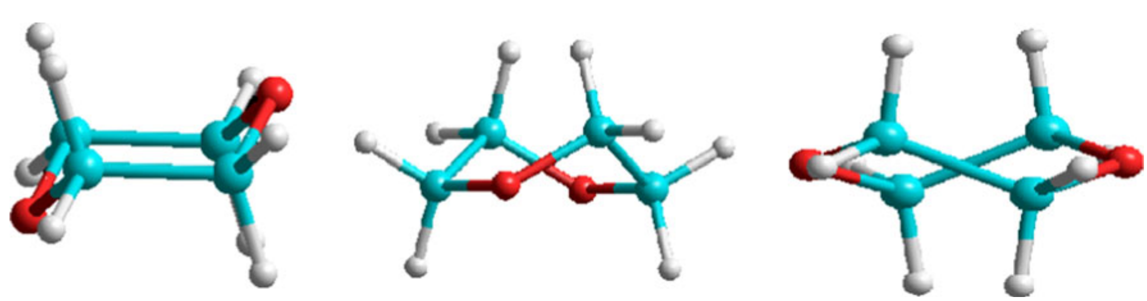

Fig. 1 Examples of the chair, 2,5 twist-boat and 1,4 twist-boat conformers, respectively, in the molecule of 1,4-dioxane

Table 2 Dipole moment, in debyes, in gas phase, neat liquid, and water solution

Conformer	Gas phase	Neat liquid	Water solution
Chair	0.00	0.00	0.13
1,4 Twist-boat	0.00	0.06	0.12
2,5 Twist-boat	1.51	1.75	2.76

Table 3 Free energy difference, in kcal/mol, for the conversion of chair to twist-boat, in solution

	Chair → 2,5 twist-boat			Chair → 1,4 twist-boat		
	ΔE_{QM}	ΔG_{int}	ΔG	ΔE_{QM}	ΔG_{int}	ΔG
Neat liquid	6.8	0.1	6.9	6.4	0.0	6.4
Water solution	7.7	−1.2	6.5	6.6	−0.4	6.2

Given that a priori we do not know the population of the different conformers, we performed several QM/MM simulations using mixtures of different compositions. Firstly, we supposed that the simulation box was formed by one solute molecule, either in the chair conformation or in the twist-boat conformation, surrounded by 299 molecules in the chair conformation. Secondly, following Takamuku et al. [5], we assumed that liquid 1,4-dioxane is composed of a mixture formed by 65 % of chair form and 35 % of the 2,5 twist-boat form. Independently of the initial composition of the liquid, the free energy differences between the chair and the 2,5 and 1,4 twist-boat conformers were 6.9 and 6.4 kcal/mol, respectively. With these values, one can estimate the actual population of each conformer in the mixture that turns out to be 0.01 % twist-boat versus 99.99 % chair form. Therefore, it can be concluded that also in the neat liquid, almost all of the 1,4-dioxane is in the chair form. The results obtained in our work refute the results of Takamuku et al. [5] but agree with the results obtained by other authors [6, 8, 9]. It remains to clarify whether the slightly larger population (about 1 % of boat forms) obtained by Cinacchi et al. [10] is due to the use of a flexible model by these authors or to other differences in the force fields used.

After establishing that the chair form displays populations close to 100 % in both gas phase and the neat liquid and that the contribution of boat conformers seems to be negligible, we computed the vaporization enthalpy as [46]:

$$H = \frac{1}{2}(E_{elect} + E_{LJ}) + E_{dist} + RT \qquad (8)$$

Here, E_{elect} is the solute–solvent electrostatic interaction energy that is calculated using the polarized charge distribution of the molecules, E_{LJ} is the Lennard-Jones interaction energy, and E_{dist} is the energy spent in polarizing the electron distribution and distorting the geometry of the dioxane molecule from gas to liquid phase. The vaporization enthalpy for the chair isomers obtained with the ASEP/MD method was 8.9 kcal/mol, where we have assumed that all the molecules are in the chair conformation. This enthalpy value agrees well with the experimental value, 9.2 kcal/mol [10]. The values obtained for the different contributions E_{elect}, E_{LJ}, and E_{dist} of the vaporization enthalpy were −2.8, −13.9, and +0.1 kcal/mol, respectively. Clearly, the interaction energy is dominated by the LJ component. The electrostatic contribution represents only 17 % of the total interaction energy. The extremely low value of the distortion energy evidences that the geometry and wave function of the dioxane molecule in its chair conformation are hardly affected by the environment.

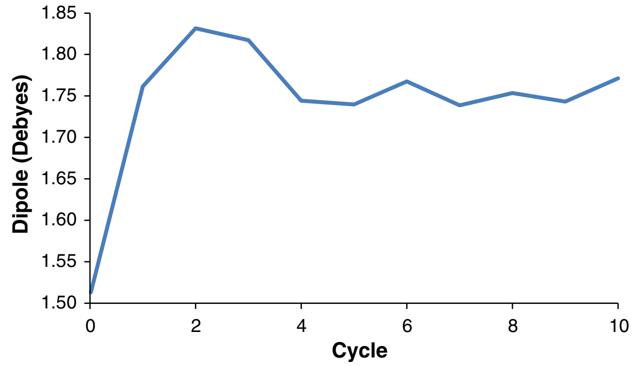

Fig. 2 Evolution of the solute dipole moment, in debyes, versus the number of ASEP/MD cycles

Next, we pass to describe the solvent effect on the charge distribution of the molecule. Figure 2 shows the evolution of the dipole moment of the 2,5 twist-boat conformer during the ASEP/MD process. Initially, the dipole moment increases as the molecule gets polarized until it reaches the equilibrium value and then it begins to fluctuate. In previous papers [17–21], it was shown that the size of the fluctuations is related to the finite length of the MD simulations (the same fact explains why the chair and 1,4 twist-boat forms display non-null dipole moments in some cases, when symmetry would require a null dipole). The dipole moment of the 2,5 twist-boat increases from 1.51 to 1.75 D. This increase in the dipole moment is parallel to the redistribution of the atomic charges. As a general trend and for the three isomers, there is a flux of charge from carbon atoms to hydrogen atoms during the passage from gas phase to liquid, see Table 4. It is worth noting that the charge on the carbon atoms become almost null in solution, while the charge on the hydrogen atoms increase. Consequently, the center of positive charge moves away from the oxygen atoms, thus explaining the increase in the dipole moment in the 2,5 twist-boat form.

Table 4 Atomic charges for 1,4-dioxane

Atom	Chair			2,5 Twist-boat			1,4 Twist-boat		
	Gas phase	Neat liquid	Water solution	Gas phase	Neat liquid	Water solution	Gas phase	Neat liquid	Water solution
C	0.119	0.003	0.053	0.207	0.069	0.173	0.151	0.017	0.149
O	−0.381	−0.351	−0.509	−0.408	−0.370	−0.558	−0.412	−0.380	−0.573
H_{equat}	0.033	0.083	0.093	−0.019	0.070	0.043	0.015	0.061	0.044
H_{axial}	0.038	0.089	0.109	0.016	0.046	0.063	0.035	0.096	0.082

Table 5 Bond lengths, in Å, for 1,4-dioxane

Bond	Chair			2,5 Twist-boat			1,4 Twist-boat		
	Gas phase	Neat liquid	Water solution	Gas phase	Neat liquid	Water solution	Gas phase	Neat liquid	Water solution
C–O	1.424	1.425	1.433	1.424	1.425	1.433	1.429	1.430	1.438
C–C	1.519	1.518	1.513	1.530	1.529	1.526	1.516	1.514	1.509
C–H_{equat}	1.090	1.090	1.089	1.095	1.097	1.093	1.096	1.096	1.094
C–H_{axial}	1.098	1.097	1.095	1.092	1.090	1.090	1.091	1.091	1.090

4.2.2 Structure

The geometries of both solute and solvent molecules were optimized in solution at exactly the same level of calculation used in gas phase, i.e., B3LYP/aug-cc-pVTZ. In addition to the solute geometry, we also analyze the solvent structure around it.

Regarding the solute geometry, and as a general trend, the changes in bonds lengths and angles when moving from gas phase to solution are somewhat larger in the boat form than in the chair form. In any case, the variations are small. When the dioxane molecule passes from gas phase to the neat liquid, the C–O distances increase but the C–C and C–H_{axial} bond lengths decrease (Table 5). The decrease in the C–H_{axial} distances is compatible with the formation of a C–H–O hydrogen bond in the liquid. In fact, it has been hypothesized that C–H–O hydrogen bonds induce a contraction of the C–H bond, which is the opposite of the effect found for conventional O–H donor bonds. As expected, this bond length shortening translates into a blue shift of the calculated vibrational frequencies of the modes that involve the C–H_{axial} bonds, increasing from 2966, 2973, 2979, and 2983/cm in gas phase to 2973, 2979, 2985, and 2989/cm in the neat liquid.

Next, we analyze the structure of the liquid assuming that in its composition enters only the chair conformer. The main question to clarify is the possible existence of C–H–O hydrogen bonds. Figure 3 shows the center of mass pair intermolecular radial distribution function, RDF, in the neat liquid. The RDFs were obtained by averaging the 5 last molecular dynamics simulations in the corresponding ASEP/MD calculation.

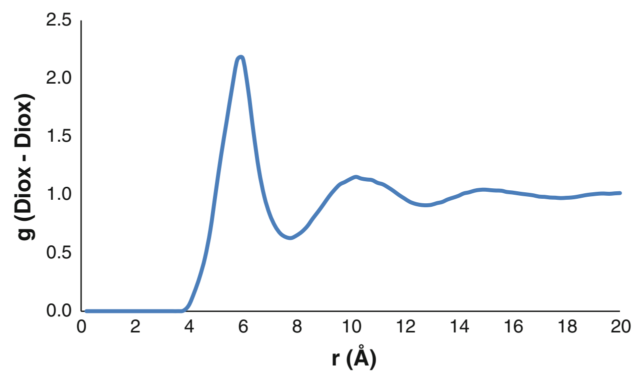

Fig. 3 Radial distribution function corresponding to the centers of mass of the 1,4-dioxane chair molecules

There is a very well-defined first peak at 5.8 Å. Integration of the peak permits to obtain the first shell coordination number that turns out to be 12, which is characteristic of compact packing. There is a second peak, corresponding to the second solvation layer at about 10 Å and even the third solvation layer can be seen about 15 Å. This RDF is characteristic of a Lennard-Jones liquid. Next, the O_{Diox}–H_{Diox} radial distribution functions for axial and equatorial hydrogen atoms, Fig. 4, were analyzed. The RDF of equatorial hydrogen atoms is structureless but in the case of the axial hydrogen atoms there is a well-defined peak at about 6 Å that coincides with the distance between the centers of mass.

It is worth noting the shoulder in the RDFs at 2.8 Å. In order to clarify its origin, hydrogen density maps around the dioxane molecule are displayed. Figure 5a shows that hydrogen atoms are concentrated mainly near

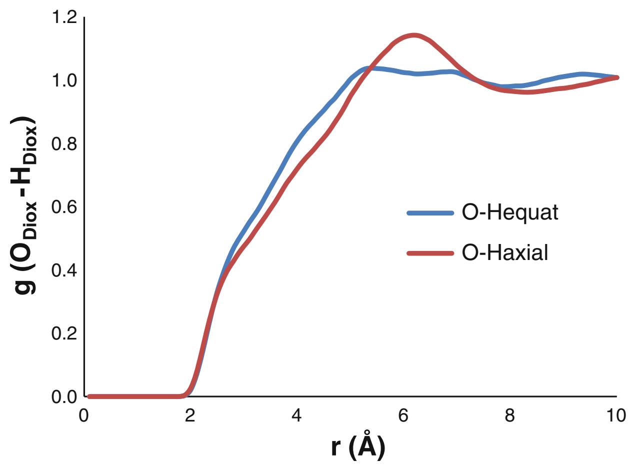

Fig. 4 Radial distribution functions corresponding to the pair O_{Diox}–H_{Diox}

the free electron pairs of oxygen atoms of the molecule of 1,4-dioxane. There are high-concentration regions at 2.8 Å. Tentatively, one can assign the shoulder to the formation of C–H–O HBs. Figure 5b displays the position of the oxygen atoms around the dioxane molecule. The high concentration above and under the molecule is due to oxygen atoms interacting with the axial hydrogen atoms. The distance between the hydrogen and the area of high concentration of oxygen atoms is again 2.8 Å. No equivalent structures are found around the equatorial hydrogen atoms. All these facts taken together point to (1) the presence of C–H–O HBs at a distance of 2.8 Å and (2) a preference for the oxygen atoms to interact with axial hydrogen atoms. However, the absence of a clear peak in the O_{Diox}–H_{Diox} RDF at 2.8 Å and the low value of the isodensity used in generating Fig. 5 clearly indicate that this atypical hydrogen bond is too weak to create a well-defined solvent structure around the solute.

4.3 Water solution

In aqueous solution, since we have a polar solvent, both the chair and boat conformers experience greater polarization than in the neat liquid. So, the dipole moment becomes 2.76 D for the 2,5 twist-boat conformer. Unexpectedly, this increase in the dipole moment has no influence on the relative stability of the conformers in aqueous solution. In fact, the results are completely equivalent to those obtained in the neat liquid. The free energy differences between the chair and the 2,5 and 1,4 twist-boat forms turn out to be 6.5 and 6.2 kcal/mol, respectively. Consequently, also in aqueous solution, the only conformer that has a non-negligible population is the chair form.

Given that the 2,5 twist-boat form shows a higher value of the dipole moment, one would expect it to interact more strongly with the solvent and therefore to experience a higher stabilization than the chair form, something that does not occur. With the aim to clarify this point, Table 3 displays different contributions to the free energy difference in neat liquid and in water solution. In the two cases, the main contribution to the stability comes from the internal energy, ΔE_{QM}. As expected, the solute–solvent interaction energy is larger in water than in dioxane due to the larger value of the water dielectric constant and to the formation of a strong hydrogen bond between the water and dioxane molecules, see below. In the neat liquid, the two components of the free energy (internal and solute–solvent interaction) favor the formation of the chair conformer, in water both components work in opposite directions, see Table 3.

As expected, and in agreement with the results of Pchelkim and Toryamk [12], the twist-boat conformer displays somewhat larger solute–solvent interaction energy than the chair conformer. As a consequence, the free energy difference between chair and boat conformers slightly decreases in water solution. However, this decrease

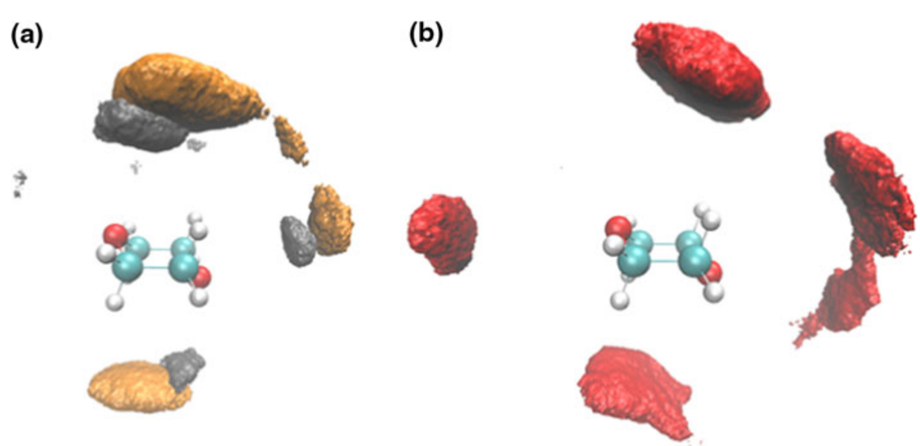

Fig. 5 Occupancy maps of 1,4-dioxane, considered as CPK spheres, as calculated by VMD [47]: **a** hydrogen (*gray*) and carbon (*golden*) atoms; **b** oxygen (*red*) atoms

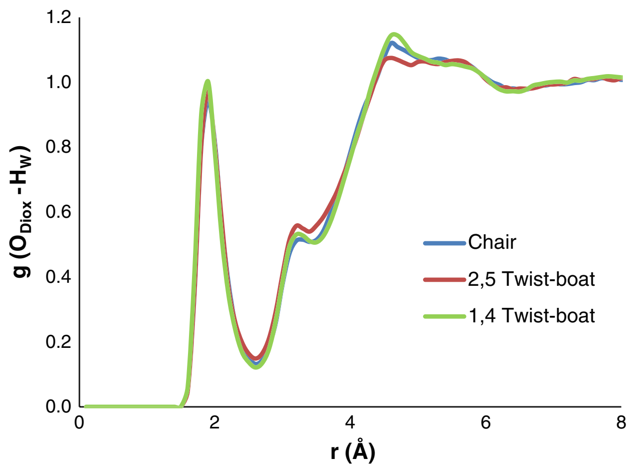

Fig. 6 Radial distribution function corresponding to the O_{Diox}–H_W pair (solute oxygen and solvent hydrogen)

is compensated in part by the increase in the internal energy, and consequently, there are no appreciable changes in the relative populations. The explanation to the fact that both twist-boat and chair conformers display similar interaction energies is that, despite the differences in the total dipole moments, both structures have similar charge distributions. The higher electronic density in oxygen atoms produces similar partial dipole moments, but while in the chair conformer both partial dipoles point in opposite directions, which produces a null total moment, in the 2,5 twist-boat conformer the two dipoles form an angle close to 116°, leading to a significant total dipole moment.

Figure 6 shows the O_{Diox}–H_w intermolecular RDFs. For the calculation of the RDF, the last 5 steps of the molecular dynamics in the corresponding ASEP/MD calculation were used. Chair and twist-boat conformers have a similar behavior. In the three conformers, there are very well-defined peaks at around 1.9 Å corresponding to intermolecular hydrogen bonds dioxane-water. Given the difference in dipole moments between the three conformers, it is clear that it is the hydrogen bond network that mainly determines the solvent structure and not the total dipole moments of the molecules.

Figure 7 displays the occupancy maps of water hydrogen atoms around 1,4-dioxane. As expected, hydrogen atoms of water molecules are located near the oxygen atoms of the solute molecule forming strong O_{Diox}-H_w hydrogen bonds at a distance of 1.9 Å. More interesting, Fig. 7 displays also the occupancy maps of water oxygen atoms. In addition to the already mentioned O_{Diox}–O_w hydrogen bonds, there are also high-concentration regions of oxygen atoms at 2.8 Å, as in the neat liquid this points to the presence of C–H–O(w) HBs. It is noteworthy the preference for water molecules to form HB with axial hydrogen atoms instead of equatorial hydrogen atoms. This behavior contrasts with the results obtained in small

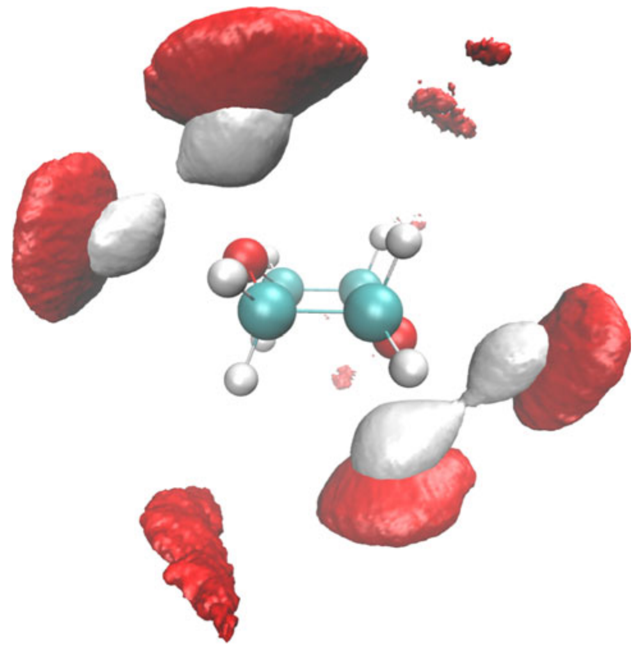

Fig. 7 Occupancy maps of water hydrogen (*gray*) and oxygen (*red*) atoms (considered as CPK spheres, as calculated by VMD) [47] around 1,4-dioxane

clusters formed by dioxane and two or three water molecules where the contrary is found [13]. The explanation to this fact is that in gas phase clusters, only those structures that involve the equatorial hydrogen atoms permit the two water molecules bonded to the oxygen and hydrogen atoms of dioxane to form a HB between them. This restriction is not present in the solution where water can form much more extended networks.

The changes in the dioxane bond lengths found in water solution are similar to those in the neat liquid. The C–H bond lengths decrease more in the axial hydrogen than in the equatorial atoms, confirming the preference of solvent to form HBs with the former. These non-conventional HBs are probably responsible for the small shoulder in the H_{axial}–O_w RDF at 2.8 Å (see supplementary information).

4.3.1 *Comparison with IEF-PCM calculations*

In this section, we compare the results obtained with ASEP/MD and continuum dielectric models. Although PCM neglects completely the contribution of specific interactions, hydrogen bonds for instance, it yields to results that, in many cases, are comparable to those of more sophisticated methods. Here, we compare the performance of both methods in the prediction of several properties: relative populations of the conformers in the neat liquid and in aqueous solution, HOMO–LUMO gap energy, and position of the first band of the vis-UV absorption spectrum.

With respect to the conformational equilibrium in the neat liquid, IEF-PCM provides for the free energy difference between the chair and 2,5 twist-boat conformers a value of 6.8 kcal/mol. This result is only slightly larger than that provided by ASEP/MD, 6.4 kcal/mol. As we have shown above, specific interactions play only a marginal role in the conformational equilibrium of dioxane in the pure liquid, and consequently, the two methods provide similar results.

The relative stability in water of the two twist-boat conformers compared with the chair conformer was 6.5 kcal/mol for the 2,5 twist-boat and 6.3 kcal/mol for the 1,4 twist-boat, almost identical to the ASEP/MD values. This result is striking because now specific interactions play an important role. There are strong hydrogen bonds between dioxane and water. However, as shown in Fig. 6, the O_{Diox}–H_w RDFs are completely equivalent in chair and twist-boat forms; therefore, the two conformers form similar hydrogen bonds with water. Consequently, the contribution of specific interactions to the stability of the different conformers is similar, canceling out when the free energy difference between them is calculated. It is worth noting that the electrostatic interaction energies are, however, very different when calculated with IEF-PCM, −5.6 and −6.3 kcal/mol for the chair and boat conformers, respectively, and with ASEP/MD, −21.7 and −23.7 kcal/mol. Clearly, IEF-PCM underestimates the solute–solvent interaction energy. So, we can conclude that IEF-PCM and QM/MM methods provide similar results when one studies systems in which hydrogen bonds play a marginal role or in those cases where, despite being important, their number remains constant. On the contrary, one would expect that continuum models fail in the description of processes where specific interactions play an important role and, furthermore, the solute–solvent interaction energies change. To illustrate this, we compare the results obtained for the HOMO–LUMO energy gap and the position of the first band of the electron absorption spectrum. Table 6 provides the values for the HOMO and LUMO energies and the HOMO–LUMO gap in the three phases considered. The HOMO energy decreases in 0.03 eV when one passes from gas phase to the neat liquid but increases in about 0.25 eV in aqueous solution. This latter value decreases to 0.10 eV when calculated with IEF-PCM. Regarding the H–L gap, this is 6.57 eV in gas phase, 6.75 eV in water solution using IEF-PCM, and 7.29 when specific interactions are included with ASEP/MD. Clearly, continuum models yield only a reduced percentage of the total H–L gap.

Finally, Table 7 displays results for the position of the first band of the electronic absorption spectrum of 1,4-dioxane calculated using TD-DFT. In gas phase, the experimental [48] absorption maximum is centered at 6.88 eV. B3LYP provides a value of 6.17 eV. The agreement with the experiment is improved when the CAM-B3LYP functional is used. In this case, we get a value of 6.81 eV. In dioxane liquid, where there are no strong hydrogen bonds, PCM and ASEP/MD provide very similar values. However, in water solution, both methods yield very different results: PCM provides a value for the transition energy that is 0.6 eV lower than the ASEP/MD value independently of the functional used. With CAM-B3LYP and PCM, the gas phase water solvent shift is estimated as about 0.14 eV, while ASEP/MD yields 0.7 eV. In sum, dielectric continuum models can represent an alternative to more costly QM/MM methods in those cases where there are no specific interactions or when, although they are present, one is interested in calculating differences in properties or quantities where the number and strength of HB is constant; otherwise, their use is not advisable.

Table 6 Energy in eV for HOMO and LUMO orbitals and HOMO-LUMO gap for 1,4-dioxane in its chair conformation

	Gas phase	ASEP/MD		IEF-PCM	
		Neat liquid	Water solution	Neat liquid	Water solution
HOMO	−6.80	−6.77	−7.05	−6.82	−6.90
LUMO	−0.23	−0.11	0.24	−0.18	−0.15
H–L gap	−6.57	−6.66	−7.29	−6.64	−6.75

Table 7 Electronic transition, in eV, for 1,4-dioxane

	Gas phase	ASEP/MD		IEF-PCM	
		Neat liquid	Water solution	Neat liquid	Water solution
B3LYP	6.17	6.30	6.99	6.25	6.39
CAM-B3LYP	6.81	6.91	7.51	6.89	6.95

5 Conclusions

In this work, the properties of 1,4-dioxane in gas phase, neat liquid, and dilute aqueous solution were studied. Regarding the relative stability of the studied conformers, some conclusions can be drawn. Firstly, in all the cases, the population of the twist-boat conformers was less than 0.01 %. The main factor that determines the conformational equilibrium is the internal energy of the dioxane molecule. The solute–solvent interaction energy represents only a small fraction of the total free energy despite the great differences in the dipole moment values of the different isomers. The reason is that the hydrogen bond network, which determines the solvent structure, and the charge distribution, which determines the partial dipole moment over each oxygen atom, are quite similar in chair and twist-boat conformers. Secondly, the explicit consideration of the solute polarization, although it modifies the solute charge distribution of the dioxane molecule, hardly has any effect on the final free energies, as the polarized charge distributions are very similar in the different conformers.

The existence of C–H–O hydrogen bonds in the neat liquid and in aqueous solution is revealed by the presence of a shoulder in the H_{Diox}–O_w RDF and more clearly by the occupancy maps of water oxygen atoms around the 1,4-dioxane molecule. Our results support IR and Raman data that point to these interactions as responsible of the shortening of the C–H bond lengths. The large H–O distance, about 2.8 Å, is characteristic of a very weak HB, and it explains the small effect that they have on the liquid structure, which can be described as a Lennard-Jones liquid. Our calculations show that there is a preference of solvent molecules to interact with axial hydrogen atoms, in contrast with the results of small dioxane-water clusters where interaction with the equatorial hydrogens is preferred.

Finally, we compared the results obtained with dielectric continuum methods and with ASEP/MD. The main advantage of continuum methods is their simplicity and low computational cost and its main handicap is the complete neglect of the microscopic structure of the solvent, something that a priori can be very important in associated liquids. Unexpectedly, we found that this method provided correct conformational free energy differences even in aqueous solution. However, the solute–solvent interaction energies provided by continuum and ASEP/MD methods are significantly different. The dielectric continuum method fails to reproduce HOMO–LUMO energy gaps and electron transition energies in water but not in dioxane. So, its use is not advisable in the study of processes where the strength or the number of hydrogen bonds changes. On the contrary, ASEP/MD permits to include specific interactions and yields correct results in all situations, independently of the nature of the liquid and process studied.

Acknowledgments This work was supported by the Gobierno de Extremadura and the European Social Fund.

References

1. Yang TC, Ning CG, Su GL, Deng JK, Zhang SF, Ren XG, Huang YR (2006) Chin Phys Lett 23:1157–1160
2. Senthilkumar K, Kolandaivel P (2003) Comput Biol Chem 27: 173–183
3. Pickett LW, Hoeflich NJ, Liu TC (1951) J Am Chem Soc 73:4865–4869
4. Mizuno K, Imafuji S, Fujiwara T, Ohta T, Tamiya Y (2003) J Phys Chem B 107:3972–3978
5. Takamuku T, Yamaguchi A, Tabata M, Yoshida K, Wakita H, Yamaguchi T (1999) J Mol Liq 83:163–177
6. Ahn-Ercan G, Krienke H, Schmeer G (2006) J Mol Liq 129: 75–79
7. Chapman DM, Hester RE (1997) J Phys Chem A 101:3382–3387
8. Nagy PI, Volgyi G, Takacs-Novak K (2008) J Phys Chem B 112:2085–2094
9. Krienke H, Ahn-Ercan G, Barthel J (2004) J Mol Liq 109: 115–124
10. Cinacchi G, Ingrosso F, Tani A (2006) J Phys Chem B 110:13633–13641
11. Takamuku T, Yamaguchi A, Matsuo D, Tabata M, Yamaguchi T, Otomo T, Adachi T (2001) J Phys Chem B 105:10101–10110
12. Pchelkin VN, Toryanik AI (1991) Zh Strukt Khim 32(2):88–97
13. Chang HC, Jiang JC, Chuang CW, Lin JS, Lai WW, Yang YC, Lin SH (2005) Chem Phys Lett 410:42–48
14. Fdez. Galván I, Sánchez ML, Martín ME, Olivares del Valle FJ, Aguilar MA (2003) Comput Phys Commun 155:244–259
15. García Prieto FF, Fdez-Galván I, Aguilar MA, Martín ME (2011) J Chem Phys 135:194502–194510
16. Corchado JC, Sánchez ML, Aguilar MA (2004) J Am Chem Soc 126:7311–7319
17. Sánchez ML, Martín ME, Aguilar MA, Olivares del Valle FJ (2000) J Comput Chem 21:705–715
18. Martín ME, Sánchez ML, Olivares del Valle FJ, Aguilar MA (2002) J Chem Phys 116:1613–1620
19. Sánchez ML, Martín ME, Fdez Galván I, Olivares del Valle FJ, Aguilar MA (2002) J Phys Chem B 106:4813–4817
20. Fdez. Galván I, Sánchez ML, Martín ME, Olivares del Valle FJ, Aguilar MA (2003) J Chem Phys 118:255–263
21. Fdez. Galván I, Martín ME, Aguilar MA (2004) J Comput Chem 25:1227–1233
22. Sánchez ML, Aguilar MA, Olivares del Valle FJ (1997) J Comput Chem 18:313–322
23. Aguilar MA, Sánchez ML, Martín ME, Fdez. Galván I (2007) An effective hamiltonian method from simulations: ASEP/MD. In: Mennucci, B, Cammi R (eds) Continuum solvation models in chemical physics, 1st edn. Wiley, West Sussex, England, chapter 4.5, pp 580–592
24. Warshel A, Levitt M (1976) J Mol Biol 103:227–249
25. Field MJ, Bash PA, Karplus M (1990) J Comput Chem 11:700–733
26. Luzhkov V, Warshel A (1992) J Comput Chem 13:199–213
27. Gao J (1992) J Phys Chem 96:537–540
28. Vasilyev VV, Bliznyuk AA, Voityuk AA (1992) Int J Quantum Chem 44:897–930

29. Théry V, Rinaldi D, Rivail JL, Maigret B, Ferenczy GG (1994) J Comput Chem 15:269–282
30. Thompson MA, Glendening ED, Feller D (1994) J Phys Chem 98:10465–10476
31. Muñoz Losa A, Fdez. Galván I, Martín ME, Aguilar MA (2006) J Phys Chem B 110:18064–18071
32. Chandrasekhar J, Smith SF, Jorgensen WL (1985) J Am Chem Soc 107:154–163
33. Chandrasekhar J, Jorgensen WL (1985) J Am Chem Soc 107:2974–2975
34. Jorgensen WL (1989) Acc Chem Res 22:184–189
35. Okuyama-Yoshida N, Nagaoka M, Yamabe T (1998) Int J Quantum Chem 70:95–103
36. Wei D, Salahub DR (1994) Chem Phys Lett 224:291–296
37. Tuñón I, Martins-Costa MTC, Millot C, Ruiz-López MF, Rivail JL (1996) J Comput Chem 17:19–29
38. Wesolowski TA, Warshel A (1993) J Phys Chem 97:8050–8053
39. Wesolowski TA, Muller RP, Warshel A (1996) J Phys Chem 100:15444–15449
40. Jorgensen WL, Chandrasekhar J, Madura JD, Impey RW, Klein ML (1983) J Chem Phys 79:926–935
41. Frisch MJ, Trucks GW, Schlegel HB, Scuseria GE, Robb MA, Cheeseman JR, Scalmani G, Barone V, Mennucci B, Petersson GA, Nakatsuji H, Caricato M, Li X, Hratchian HP, Izmaylov AF, Bloino J, Zheng G, Sonnenberg JL, Hada M, Ehara M, Toyota K, Fukuda R, Hasegawa J, Ishida M, Nakajima T, Honda Y, Kitao O, Nakai H, Vreven T, Montgomery JA Jr, Peralta JE, Ogliaro F, Bearpark M, Heyd JJ, Brothers E, Kudin KN, Staroverov VN, Kobayashi R, Normand J, Raghavachari K, Rendell A, Burant JC, Iyengar SS, Tomasi J, Cossi M, Rega N, Millam JM, Klene M, Knox JE, Cross JB, Bakken V, Adamo C, Jaramillo J, Gomperts R, Stratmann RE, Yazyev O, Austin AJ, Cammi R, Pomelli C, Ochterski JW, Martin RL, Morokuma K, Zakrzewski VG, Voth GA, Salvador P, Dannenberg JJ, Dapprich S, Daniels AD, Farkas Ö, Foresman JB, Ortiz JV, Cioslowski J, Fox DJ (2009) Gaussian 09. Gaussian Inc., Wallingford, CT
42. Refson K (2000) Comput Phys Commun 126:310–329
43. Chirlian LE, Breneman CM, Francl MM (1987) J Comput Chem 8:894–905
44. Breneman CM, Wiberg KB (1990) J Comput Chem 11:361–373
45. Tomasi J, Mennucci B, Cammi R (2005) Chem Rev 105:2999–3094
46. Martín ME, Sánchez ML, Olivares del Valle FJ, Aguilar MA (2002) J Chem Phys 116(4):1613–1620
47. Humphrey W, Dalke A, Schulten K (1996) J Mol Graph 14:33–38
48. Hernandez GJ, Duncan ABF (1962) J Chem Phys 36:1504–1508